9108 *Macromolecules* **2010**, *43*, 9108–9116
DOI: 10.1021/ma1014462

Macromolecules
ARTICLE

Probing Nanometer-Thick Polyelectrolyte Layers Adsorbed on Oppositely Charged Particles by Dynamic Light Scattering

José Hierrezuelo, Istvan Szilagyi, Andrea Vaccaro, and Michal Borkovec*

Department of Inorganic, Analytical, and Applied Chemistry, University of Geneva, Sciences II, 30, Quai Ernest-Ansermet, 1211 Geneva 4, Switzerland

Received June 30, 2010; Revised Manuscript Received September 20, 2010

ABSTRACT: The thickness of adsorbed polyelectrolyte layers on oppositely charged particles can be measured by dynamic light scattering (DLS) with a precision of fractions of a nanometer. However, such data can be only reliably obtained when effects of particle aggregation are carefully eliminated by working at low particle number concentrations. In order to achieve a sufficient light scattering intensity at the same time, the size of colloidal particles must be chosen relatively large. We find that such measurements are best carried out with latex particles in the range of diameters of 150−300 nm. The precision of the measurement can be further enhanced with multiangle DLS. The thickness of adsorbed polyelectrolyte layers on oppositely charged particles is normally below 10 nm. At low ionic strengths, a typical thickness is merely 1−2 nm, while at higher ionic strengths one observes thicknesses between 6 and 9 nm. The transition between these two regimes occurs at ionic strengths 0.01−0.05 M. These observations were made with various highly charged cationic and anionic polyelectrolytes and can be considered as quite generic.

1. Introduction

Adsorption of polyelectrolytes on colloidal particles is essential in numerous applications, including wastewater treatment, papermaking, or suspension stabilization.[1−4] More recently, polyelectrolyte capsules obtained by layer-by-layer deposition of oppositely charged polyelectrolytes on colloidal particle templates incited substantial interest as responsive delivery systems.[5−7] Given the importance of polyelectrolyte adsorption in all these applications, reliable techniques to characterize adsorbed polyelectrolyte layers on colloidal particles are essential.

Depletion and electrokinetic techniques provide detailed information on the adsorbed mass of polyelectrolytes on oppositely charged colloidal particle surfaces.[8−16] These studies indicate that the adsorbed mass is relatively low, typically below 2 mg/m^2. The adsorbed mass generally increases with increasing ionic strength, and this trend suggests the progressive screening of electrostatic repulsion between the chains. With decreasing line charge density of the polyelectrolyte, a maximum in the adsorbed mass has been reported.[8,13,17]

Obtaining information on the internal structure of the adsorbed layer is less straightforward. The simplest additional structural parameter is the layer thickness. Small-angle neutron scattering (SANS) contrast variation experiments provide information on the layer thickness and the adsorbed amount simultaneously.[6,18−24] Such experiments suggest that the adsorbed layer of highly charged polyelectrolyte poly(diallyldimethylammonium chloride) (PDADMAC) of a molecular mass of 450 kg/mol has a thickness of 0.8 nm on oppositely charged latex particles.[18] Comparison of this value to the corresponding adsorbed amount reveals that the layer is moderately compact, whereby the polymer occupies a volume fraction of 31%. These findings are consistent with SANS studies on thicker polyelectrolyte multilayers adsorbed on colloidal particles.[6] The cited study reports an average layer thickness per single polyelectrolyte layer of 1.6 nm. When interpreting such results, one should keep in mind that adsorbed polyelectrolyte layers may also be laterally heterogeneous.[25−27] The above discrepancy of about a factor of 2 could be related to such heterogeneities.

SANS was extensively used to study adsorbed layers of poly(ethylene oxide) (PEO) on colloidal particles.[19−23] This neutral water-soluble polymer adsorbs in somewhat thicker layers, with a typical thickness in the range of 3−5 nm for PEO of a molecular mass of about 100 kg/mol. Small-angle neutron and X-ray scattering were equally useful to characterize grafted polymer brushes on colloidal particles.[28−31] However, such brushes are substantially thicker than adsorbed polymer layers, and their structure appears rather different from adsorbed polyelectrolyte monolayers.

Dynamic light scattering (DLS) represents another popular approach to estimate the thickness of adsorbed polymer layers. This technique appears to give reliable estimates for adsorbed layers of neutral polymers.[22,32−35] Typical hydrodynamic layer thickness for adsorbed neutral PEO of a molecular mass of 100 kg/mol lies within the range of 10−20 nm. The hydrodynamic thickness is about 3 times as large as the values obtained from SANS, but this discrepancy can be explained with the presence of a few long loops protruding into the solution.[21,22] The hydrodynamic thickness of PEI layers increases strongly with the molecular mass.[32]

Layer thicknesses of adsorbed polyelectrolytes on oppositely charged particles measured by DLS span more than 2 orders of magnitude.[9,11,13,18,24,36,37] How to reconcile these vastly different values, especially the large thicknesses up to 100 nm, with the relatively low adsorbed amounts established by other techniques remains unclear. Alternative techniques giving access to the hydrodynamic layer thickness, such as viscosity measurement or electro-optical techniques, point rather toward very thin layers with a thickness of a few nanometers.[14,38] However, these techniques are less popular, probably due to their indirect nature.

*Corresponding author: Ph + 41 22 379 6053; e-mail michal.borkovec@unige.ch.

 Published on Web 10/06/2010

Adsorbed polyelectrolyte layers have also been investigated on planar substrates in some detail.[39−45] Powerful surface-sensitive techniques became recently available to obtain information on the adsorbed mass and layer thickness for such substrates. These two parameters can be obtained independently for sufficiently thick films by ellipsometry or dual polarization interferometry (DPI).[39−41] To resolve these parameters, ellipsometry requires films that are typically thicker than 20 nm, while thinner films appear to be sufficient for DPI. Adsorbed mass and layer thickness can be also determined by combining an optical technique, such as ellipsometry or reflectometry with the quartz crystal microbalance (QCM).[42−45] Since the latter technique measures the mass of the film with the trapped solvent, a comparison with the dry mass of the polymer obtained with an optical technique yields the solvent content of the film, from which the layer thickness can be obtained. Still another approach is to use direct force measurements to infer the thickness of an adsorbed polyelectrolyte layer from the onset of short-ranged repulsive forces.[46−48]

All these techniques demonstrate that the adsorbed amount of polyelectrolytes is typically below 2 mg/m^2 on oppositely charged planar substrates.[39−41,46,49−52] The low adsorbed mass is fully in line with observations made on colloidal particles.[8−16] An increase of the adsorbed mass with increasing ionic strength and the presence of a maximum have been reported for planar substrates as well.[17,51−54] The layer thickness of adsorbed polyelectrolytes on oppositely charged planar substrates was suggested to be few nanometers.[39−41,45,46] These relatively small values indicate relatively flat and compact layers, which are in sharp contrast to the sometimes much larger values of the hydrodynamic layer thickness reported with DLS.

The purpose of this article is to show that a novel approach to perform layer thickness measurements with DLS confirms that adsorbed polyelectrolyte layers on oppositely charged particles are very thin. The essential aspect in these time-resolved measurements is to properly distinguish layer formation and particle aggregation. Particle aggregation may lead to an increase of the apparent hydrodynamic radius,[55,56] and this process complicates layer thickness measurements by DLS substantially. However, the influence of particle aggregation can be suppressed by carrying out measurements at a sufficiently low particle number concentration. Accordingly, reliable measurements of the layer thickness become routinely possible, and one obtains reproducible values which are consistently below 10 nm.

2. Experimental Section

Materials. Two types of surfactant-free sulfate latex (SL) particles were purchased from Interfacial Dynamics Corp. (Portland, OR). The smaller particles SL-A have a radius of 135 nm and a polydispersity of 5.9% as determined by transmission electron microscopy by the manufacturer and a charge density of −11 mC/m^2 as found by conductometry. The larger particles SL-B have a radius of 235 nm, a polydispersity of 2.6%, and a charge density of −49 mC/m^2. The suspensions were freed of impurities in a stirred ultrafiltration cell (Amicon 8010, Millipore, Billerica, MA) with a regenerated cellulose filter with a molecular mass cutoff 10 kg/mol (PLGC02510, Millipore). The particles were used from stock solutions of concentrations in the range 30−70 g/L.

Two cationic polyelectrolytes were used in this study. Poly(diallyldimethyl ammonium chloride) (PDADMAC) was bought from Sigma-Aldrich Chemie (409030-1 L, Steinheim, Germany) as 20% (w/w) aqueous solution. The manufacturer reports a weight-averaged molar mass of 450 kg/mol. The polydispersity index (PDI) is expected to be around 1.6 as reported earlier[57] since the synthesis procedures are similar. The polymer solution was diluted to a concentration of 0.19 g/L. Linear polyethylenimine (LPEI) with a weight-averaged molar mass about 250 kg/mol and PDI of 3.4 was obtained from Polysciences (Eppenheim, Germany). LPEI was dissolved at a concentration of about 1 g/L in 0.08 M HCl, and the sample was subsequently dialyzed with a cellulose ester membrane with a molecular mass cutoff of 10 kg/mol (No. 131270, Spectrum, Breda, The Netherlands). The polymer concentrations were verified with total carbon and nitrogen analysis (TOCV, Shimadzu). All solutions were prepared in Milli-Q water and pH 4.0 was adjusted with HCl. The desired ionic strength was obtained by adding KCl. The experiments were performed at a temperature of 25.0 ± 0.2 °C.

Electrophoretic Mobility. Electrokinetic measurements were carried out with Zetasizer Nano ZS (Malvern Instruments). Samples were prepared by mixing about 3−4 mL of water with about 0.5 mL of the appropriate electrolyte solution to obtain the desired ionic strength of 0.01 M. Subsequently, particles were added by pipeting about 1 mL from the stock solution. Finally, less than 1 mL of the polymer solution was added to the suspension to obtain the desired dose. The final volume of a sample was 5.0 mL.

Time-Resolved DLS Measurements. Light scattering experiments were performed with three different instruments. First, simultaneous measurements at several angles were carried out with the multiangle goniometer with eight photomultiplier detectors (ALV/CGS-8F, Langen, Germany) equipped with a 532 nm solid-state laser Verdi V2 operated at 0.4 W. Second, single-angle measurements at a fixed scattering angle of 90° were done with the compact goniometer system (ALV/CGS-3, Langen, Germany). Third, backscattering measurements were performed at a scattering angle of 173° with the Zetasizer Nano ZS (Malvern Instruments). The latter two instruments use a He/Ne laser operating at 633 nm as a light source and an avalanche photodiode as a detector. The sensitivity of these instruments has been tested with toluene, which yield at 90° a count rate of about 15 kHz on the multiangle instrument and 40 kHz on the single-angle instrument. The backscattering instrument yields a count rate of 350 kHz due to the much larger scattering volume. Each correlation function was accumulated for 30 s, and the apparent hydrodynamic radius was calculated with a second-order cumulant fit. Because of the low polymer concentrations, no viscosity corrections are necessary. Such measurements were repeated for 1−2 h and continued after the polymer addition for about the same period. Best values of the hydrodynamic particle radii of the bare particles are given in Table 1. The hydrodynamic layer thickness was obtained from the difference between the linear fits of the data before and after polyelectrolyte addition. These fits were carried out with a robust bisquare approach.[58] This approach was useful to eliminate outliers, which were sometimes present due to traces of dust. When no significant increase in the hydrodynamic radius was observed, the slope of the linear fit was set to zero. For graphical representation, the data were block-averaged over 40−50 data points. In a single-angle measurement, hydrodynamic radii could be typically measured with an error of about 0.3 nm, leading to an error in the hydrodynamic layer thickness of about 0.5 nm. These errors refer to a single time-dependent experimental run, and they correspond to standard deviations of the mean. These errors could be achieved at count rates of about 30 kHz or above. Lower count rates were avoided as they yielded less accurate radii within the same time window. When one compares hydrodynamic radii measured at different angles or at different solution conditions, these values were less reproducible, but they agreed within an error of 2 nm. This variation is caused by the varying scattering intensities and the different weighting by the form factor of the particles. However, the error in the layer thickness was independent of the experimental conditions used, since this number is obtained from the differences of two hydrodynamic radii obtained under same conditions.

Measurements with the goniometer systems were carried out in round borosilicate glass cuvettes cleaned with boiling mixture

Table 1. Properties of Particle−Polyelectrolyte Systems at 0.01 M KCl and pH 4

latex particles	DLS radius (nm)	polyelectrolyte	molecular mass (kg/mol)	dose at IEP (mg/g)	charging ratio (at IEP)	dose at plateau (mg/g)	reference
SL-A	144.5	PDADMAC	450	1.9	6.1	3.8	present study
SL-A	144.5	LPEI	250	0.9	5.5	1.9	present study
SL-B	238.0	PDADMAC	450	1.5	1.9	3.3	present study
SL-B	238.0	LPEI	250	0.38	1.4	0.93	present study
sulfate	96.6	PDADMAC	450	3.1	8.0	11	ref 64
amidine	110	PSS	2260	6.3	1.6	10	ref 59

of concentrated H_2SO_4 and 30% solution of H_2O_2 at volume ratio of 3:1. Backscattering measurements were performed in square 1 cm plastic cuvettes cleaned with Hellmanex solution. The cuvettes were extensively rinsed with water and dried in a dust-free environment.

The samples for layer thickness measurements were prepared in the cuvette by mixing ~0.2 mL of the particle suspension, water, and electrolyte solutions in a range of 0.2−0.8 mL to obtain the desired ionic strength. The sample was then mixed with a vortex stirrer and inserted into the light scattering instrument. After an accumulation period of 1−2 h, 20 μL of the polymer solution was added to the cuvette and the sample was gently mixed. The data accumulation was continued for a subsequent 1−2 h. The total volume of the samples was always 2 mL. The same layer thickness was observed when the volumes of the mixed solutions were comparable.

For particle aggregation measurements, the samples were prepared similarly as for the layer thickness measurements, but the particle and polymer concentrations were about 10−100 times higher. The polymer was directly added at the beginning of the measurements. Such measurements can be carried out with single-angle or multiangle instruments. The latter technique permits the determination of absolute aggregation rate constants by combining simultaneous static and dynamic measurements. The detailed experimental protocols for such measurements are given elsewhere.[12,55,56]

3. Results and Discussion

Reliable thickness measurements of adsorbed polymer layers in particle suspensions by DLS must properly distinguish between the increase in the hydrodynamic radius due to the formation of the adsorbed layer and due to particle aggregation as illustrated in Figure 1a.

Provided the particle suspension remains stable throughout the entire experiment, the measurement of the layer thickness is simple. The hydrodynamic radius R_1 of the bare particles is measured first, and this value is compared to the one in the presence of the adsorbed polymer R_2. The difference between these numbers gives the hydrodynamic layer thickness

$$L = R_2 - R_1 \quad (1)$$

The data analysis is particularly straightforward when the experiment is carried out in a time-resolved fashion, which leads to a constant baseline as indicated in Figure 1b.

When adsorbed layers of polyelectrolytes in particle suspensions of opposite charge are investigated, the particles normally aggregate at the same time. As the hydrodynamic radius is sensitive not only to the presence of an adsorbed layer but also to particle aggregates, the aggregation, and adsorption processes must be considered simultaneously. Since particle aggregation will often lead to a steady increase of the hydrodynamic radius, these two processes can be normally distinguished in a time-resolved measurement as shown in Figure 1c. The baseline will be increasing in time, possibly at different rates in the presence of the polyelectrolyte and its absence.

One might suspect that accurate layer thickness measurements require small particles in order to minimize the error originating from the difference of two large numbers in eq 1. In the case of small particles, however, a much more serious problem may originate from particle aggregation. Since aggregation is a second-order process, it can be always slowed down by dilution. At high dilutions, however, relatively large particles are necessary to obtain a sufficient light scattering signal. Therefore, layer thickness measurements should be carried out with relatively large particles, typically >100 nm in diameter.

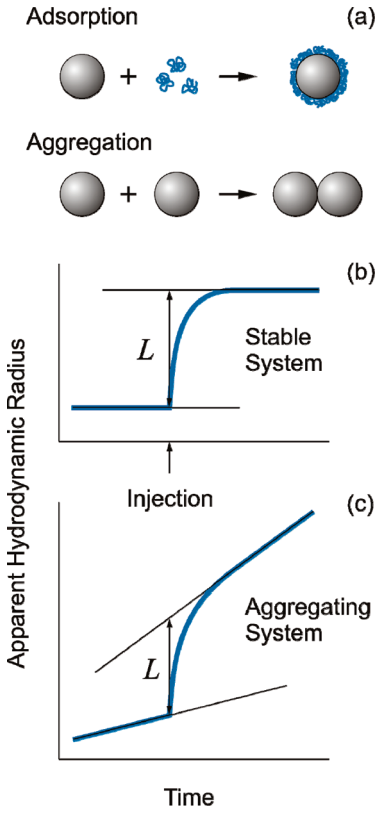

Figure 1. Adsorption of polyelectrolytes on oppositely charged particles. (a) Layer formation is often accompanied by particle aggregation. Scheme of the measurement of the hydrodynamic layer thickness L in a (b) stable and (c) aggregating system.

Charge Reversal and Particle Aggregation. Charged colloidal particles in the presence of oppositely charged polyelectrolytes are known to undergo a charge reversal process, which is also referred to as overcharging.[4,12,56,59−62] This phenomenon can be easily followed by electrophoresis. The electrophoretic mobility of the presently studied sulfate latex particles SL-A in the presence of the PDADMAC at an ionic strength of 0.01 M and pH 4.0 is shown in Figure 2a. Additional properties of the particles and polyelectrolytes used are summarized in Table 1. At low polyelectrolyte dose, the mobility is negative, which reflects the negative charge of the sulfate groups on the latex particle surface. With increasing polyelectrolyte dose, the mobility increases due to adsorption of the positively charged PDADMAC. At a dose of 1.9 mg/g, one reaches the isoelectric point (IEP), where the

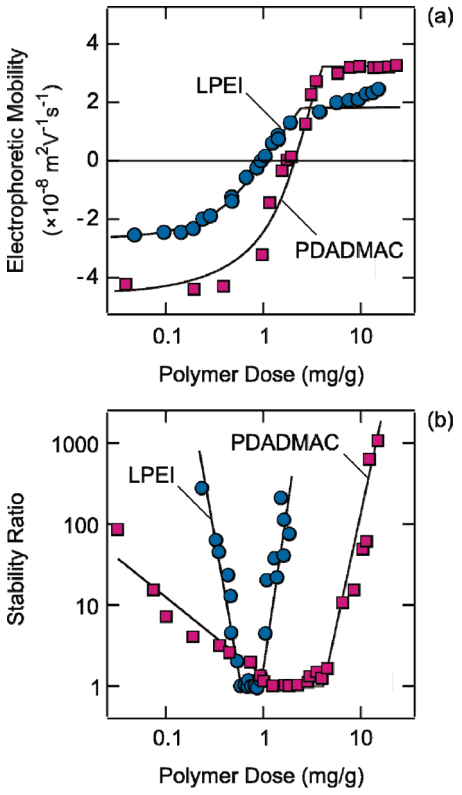

Figure 2. Typical behavior of charged colloidal particles upon addition of an oppositely charged polyelectrolyte exemplified with negatively charged latex particles SL-A at an ionic strength of 0.01 M upon addition of two different cationic polyelectrolytes, namely PDADMAC and LPEI. Solid lines serve to guide the eye only. (a) Electrophoretic mobility and (b) colloidal stability.

mobility vanishes. When the dose increases beyond this point, the mobility becomes positive since the adsorption process remains favorable in spite of the fact that the particles are now positively charged. The adsorption process saturates at a dose near 3.8 mg/g. When the dose is increased beyond this point, the adsorbed amount is constant and the excess polyelectrolyte remains dissolved in solution. At lower polyelectrolyte dose, the adsorption is quantitative.[12]

A useful parameter to characterize the IEP is the charging ratio (CR).[12] This parameter corresponds to the ratio of the number of charges of the adsorbed polyelectrolyte relative to the number of the charges on the particle. When the adsorption is stoichiometric, the CR is unity. Often, the CR exceeds unity, and in this case one refers to superstoichiometric adsorption. This situation is caused by coadsorption of the counterions of the polyelectrolyte. For the present system of PDADMAC neutralizing SL-A particles the CR is 6.1, and therefore the adsorption is superstoichiometric (see Table 1).

The colloidal stability in this system follows the electrophoresis data closely. Figure 2b shows the stability ratio for the same system. The stability ratio is the ratio of the fast aggregation rate coefficient at high ionic strength to the actual rate coefficient. One observes that the suspension is unstable near the IEP, while it becomes stable away from this point. This behavior can be rationalized as follows. Near the IEP, the surface charge is neutralized and particles aggregate rapidly due to the residual van der Waals forces. Away from the IEP, the particles develop a surface charge, which leads to the formation of an electrical double layer. The overlap of the diffuse parts of these layers leads to strong repulsive forces and to suspension stabilization.

The same phenomenon occurs with linear poly(ethylene imine) (LPEI). The data obtained with the same latex particles SL-A under at identical conditions are shown in Figure 2. Table 1 summarizes the essential parameters of the system. One observes a similar charge reversal and an unstable region close to the IEP. In this case, the dose needed to reach the IEP is 0.9 mg/g and the saturation plateau is near 1.9 mg/g. The CR of 5.5 again implies a superstoichiometric adsorption and is comparable to the PDADMAC system. One further observes that the instability region is narrower for LPEI than for PDADMAC. This feature indicates that the adsorbed PDADMAC film is more heterogeneous than the LPEI film. The lower stability of particles in the presence of PDADMAC is caused by attractive forces resulting from the patch-charge heterogeneities.[56,59,63]

Similar charge reversal has been observed for SL-B particles. The relevant parameters are summarized in Table 1. The CR is close to unity, meaning that the polyelectrolyte adsorption is almost stoichiometric. The fact that the CR is lower than for SL-A particles can be explained by the fact that the SL-B particles are more highly charged than SL-A particles. Very similar charge reversal effects have been described in other polyelectrolyte−particle systems of opposite charge earlier.[4,12,56,59−62] These studies clearly indicate that the discussed charge reversal scenario is very general, provided the charges of both particle and polyelectrolyte are sufficiently high.

Distinguishing Layer Formation from Particle Aggregation. Examples of layer thickness measurements with DLS in the presence of particle aggregation will now be presented. They will demonstrate that particle aggregation can be extremely important indeed, but they will equally indicate how reliable layer thickness measurements can be performed in aggregating systems.

The hydrodynamic radius in a rapidly aggregating suspension, which is subsequently stabilized by the addition of a polyelectrolyte, is shown in Figure 3. The experiment starts with SL-A particle suspension in 0.1 M KCl. Figure 3a,b shows the time evolution of the hydrodynamic radius for different particle concentrations. The rate of increase of the radius is fastest for the highest particle concentration of 4.6×10^{15} m^{-3} (50 mg/L) and decreases as this concentration is lowered. This behavior originates from second-order aggregation kinetics and results in an apparent rate that is proportional to the particle concentration. PDADMAC was added at a dose of 40 mg/g after 1.8 h (arrow). Since this dose is beyond the IEP, the resulting suspension is now basically stable, and the particle radius remains approximately constant.

By performing a linear fit to the time series of the particle radius before and after the polyelectrolyte injection and evaluating their difference at injection time, an estimate of the layer thickness is obtained. For the highest particle concentration, we find a value around 80 nm. When the same analysis is carried out at lower particles concentrations, this quantity decreases as shown in Figure 3c. Only at particle concentrations of 4.6×10^{13} m^{-3} (0.5 mg/L) and below one finds a constant value of 7.4 ± 0.6 nm. This number represents the valid estimate of the hydrodynamic layer thickness under these conditions. Clearly, when particle aggregation is too rapid, the increase in the particle radius is too large to obtain sufficient precision in the layer thickness measurements. By decreasing the particle concentration, particle aggregation is slowed down, making a more precise measurement of the layer thickness possible. At the same time, however, decreasing particle concentration leads to a weaker light scattering signal, making the measurements

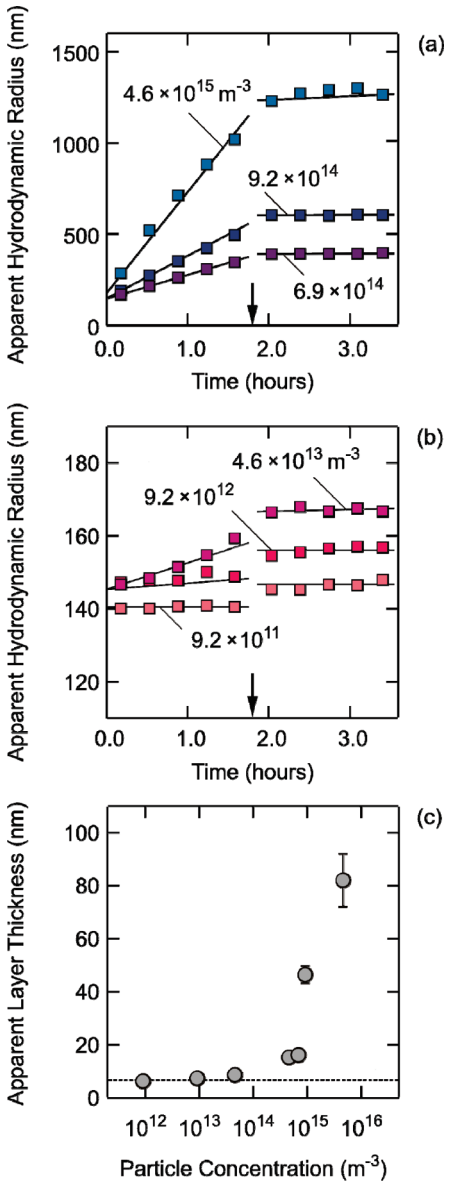

Figure 3. Layer thickness measurement in an initially aggregating suspension of SL-A latex particles at an ionic strength of 0.1 M with a subsequent addition of 40 mg/g PDADMAC (arrow). The polymer has a stabilizing effect. (a) Time dependence of the apparent hydrodynamic radius at different particle concentrations and (b) similar data for lower particle concentrations on a different scale. (c) Apparent layer thickness as a function of the particle concentration. The dotted line indicates the actual layer thickness.

of the radius less accurate. We found that reliable measurements are possible down to particle concentrations of about 3×10^{11} m^{-3} (0.003 mg/L). Clearly, the particle concentration and particle size are critical in such experiments.

Figure 4 shows similar results obtained at a lower ionic strength of 0.01 M. The particle suspension is initially stable, which results in a constant hydrodynamic radius over time. PDADMAC is added at a dose of 40 mg/g after 1.8 h (arrow). The resulting suspension is stable again, leading to a constant value of the hydrodynamic radius. Since the suspension is stable before and after the experiment, one might be tempted to think that the difference in the hydrodynamic radii represents an appropriate estimate of the layer thickness. However, variation of the particle concentration demonstrates that this reasoning is incorrect. The difference between the hydrodynamic radii decreases with the particle concentration and only reaches a

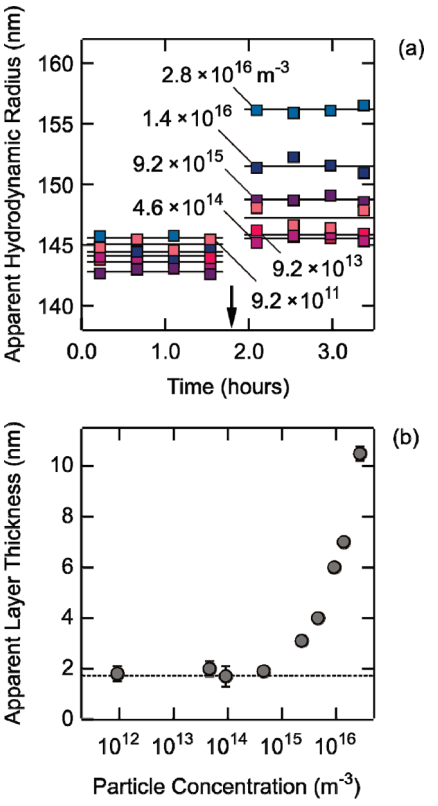

Figure 4. Layer thickness measurement in a stable suspension of SL-A latex particles at an ionic strength of 0.01 M with a subsequent addition of 40 mg/g of PDADMAC. This addition again leads to a stable suspension, but the system undergoes a transient rapid aggregation. (a) Time dependence of the apparent hydrodynamic radius of the bare particle suspension with a subsequent addition of the polyelectrolyte (arrow). (b) Apparent layer thickness as a function of the particle concentration.

plateau of 1.8 ± 0.3 nm at particle concentrations below 4.6×10^{14} m^{-3} (5 mg/L). The larger values of the apparent layer thickness at higher particle concentrations are due to particle aggregation. While the suspension is stable before and after the polymer addition, the system passes through the IEP in a transient-like fashion and becomes unstable for a short period of time. This period is sufficient for the formation of aggregates, which lead to an increase of the apparent hydrodynamic radius.

Layer thickness measurements for PDADMAC on SL-A particles are summarized in Figure 5. The corresponding results at other ionic strengths are shown together with similar measurements for the same polymer adsorbed on SL-B particles. For these particles, the particle concentration was fixed at 1.8×10^{12} m^{-3} (0.1 mg/L), and the polymer was added at a dose of 40 mg/g. Reliable measurements could be performed for the SL-B particles down to concentrations of about 5×10^{10} m^{-3} (0.003 mg/L). The data are further compared to measurements with the backscattering instrument. While the error of this technique is somewhat larger, the results are fully consistent with the goniometer data. The larger error of this technique is probably due the inferior stability of the instrument when compared to the goniometer. Because of the larger sensitivity of the backscattering instrument, however, suspensions can be studied about at 10 times lower particle concentrations than with the goniometer systems.

These findings are compatible with previous layer thickness measurements of PDADMAC films with DLS.[64] This study used the same PDADMAC sample as the one used here, but the sulfate latex particles were somewhat smaller

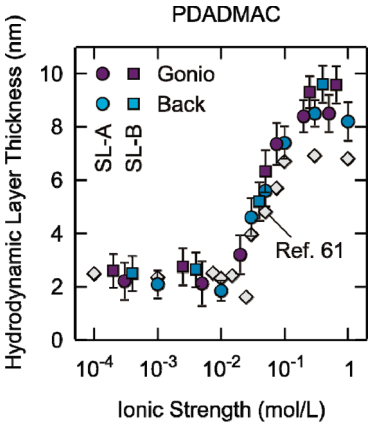

Figure 5. Hydrodynamic layer thickness of adsorbed PDADMAC as a function of the ionic strength measured with SL-A and SL-B particles at the single-angle goniometer and the backscattering instrument. The data are compared to previous layer thickness measurements carried out with the same PDADMAC sample and smaller sulfate latex particles.[64]

(see Table 1). The corresponding values at a dose 25 mg/g are shown in Figure 5. The congruence of these data sets suggests the generic nature of the phenomenon, but this aspect will be discussed in more detail below. In general, one observes an increase of the layer thickness roughly from 2 to 7 nm in a relatively narrow range of ionic strengths of 0.02−0.05 M.

Layer thickness measurements of PDADMAC adsorbed on sulfate latex particles were also carried out with DLS earlier.[36] However, these authors reported numbers which are 2−3 times larger than the ones observed here. We suspect that these numbers do not reflect the actual layer thickness as particle aggregation was probably occurring in these experiments.

These results can be further compared with SANS measurements on a similar system.[18] In these experiments, PDADMAC was also adsorbed on sulfate latex particles, but the particles were deuterated and smaller in size. The experiments were carried out at an ionic strength of about 0.01 M, and by assuming a box profile, they yielded a layer thickness of 0.8 ± 0.1 nm. At these conditions, the hydrodynamic layer thickness for the SL-A particles and the smaller particle used in the previous study[64] was 1.8 ± 0.3 nm. The discrepancy between these values is probably related to deviations from the assumed box profile or due to long loops and tails protruding into solution. Nevertheless, the reasonable agreement between these two completely independent methods confirms the consistency of the present DLS measurements.

Simultaneous Multiangle DLS. The accuracy of these measurements can be improved by simultaneous multiangle DLS. While in classical light scattering, one detector is being used to accumulate the data, modern goniometers allow simultaneous measurements at different angles. With the goniometer used in this study it is possible to perform such measurements at eight different angles. The technique thus yields data that are about 3 times more accurate than with a single detector.

Figure 6 shows such data with SL-A particles at 0.1 M ionic strength at a particle concentration of 4.6×10^{12} m^{-3} (0.05 mg/L). Even though the suspension is slowly aggregating, the suspension is diluted to the point that no appreciable increase in the particle radius is observed. LPEI was added at a dose of 600 mg/g after 1.8 h (arrow), and one observes that the hydrodynamic radius again remains stable. As shown in Figure 6b, the resulting layer thickness is independent of the

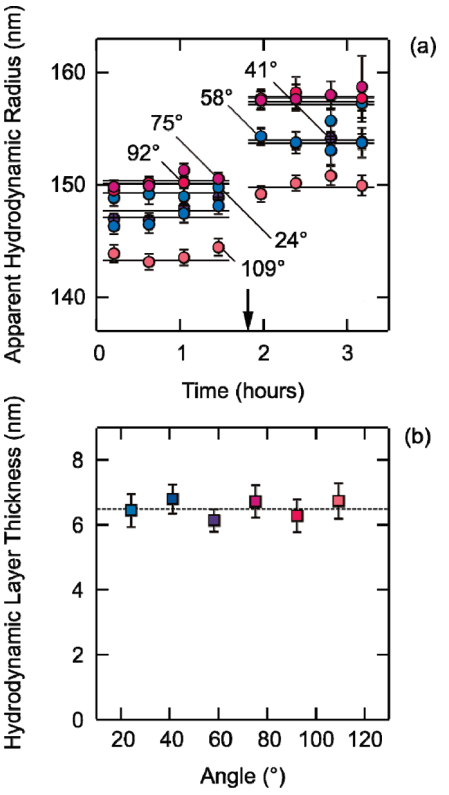

Figure 6. Layer thickness measured on multiangle goniometer in a stable suspension of SL-A latex particles at a particle concentration of 4.6×10^{12} m^{-3} (0.05 mg/L) and an ionic strength of 0.1 M with a subsequent addition of 600 mg/g LPEI. At this particle concentration, aggregation can be neglected. (a) Time dependence of the apparent hydrodynamic radius of the bare particle suspension with a subsequent addition of the polyelectrolyte (arrow). (b) Apparent layer thickness for the different angles measured.

angle, and an average value of 6.5 ± 0.2 nm is found. When only the data from detector at 92° are being used, one measures a thickness of 6.3 ± 0.5 nm. The error in the multiangle measurement is smaller indeed. The reason why only measurements at six different angles are being reported in Figure 6 is that the count rate at the two highest angles is too low due to the small form factor of the particles. Similar measurements can be carried out to particle concentrations down to 9×10^{11} m^{-3} (0.01 mg/L). The fact that this number is substantially larger than for the single-angle goniometer is mainly due the different sensitivities of the photomultiplier and the avalanche photodiode in the respective instruments.

The multiangle goniometer method can be used for thinner layers, too. Figure 7 summarizes a similar measurement with SL-A particles at the same particle concentration and an ionic strength of 0.003 M. The layer is now substantially thinner, and one finds a thickness of about 1.9 ± 0.2 nm. When the data from the detector at 92° are being used, one finds a thickness of 2.2 ± 0.5 nm. Again, the accuracy can be improved with the multiangle technique substantially.

Similar measurements were carried out at different ionic strengths. Figure 8 summarizes these findings and compares them to the conventional measurements with a single detector. The conventional approach shows a larger scatter, and the multiangle detection improves the accuracy. The data are compared with the measurements carried out on the backscattering instrument with SL-A particles. They agree with the multiangle measurements within experimental error. The error bar in the backscattering measurements is again larger,

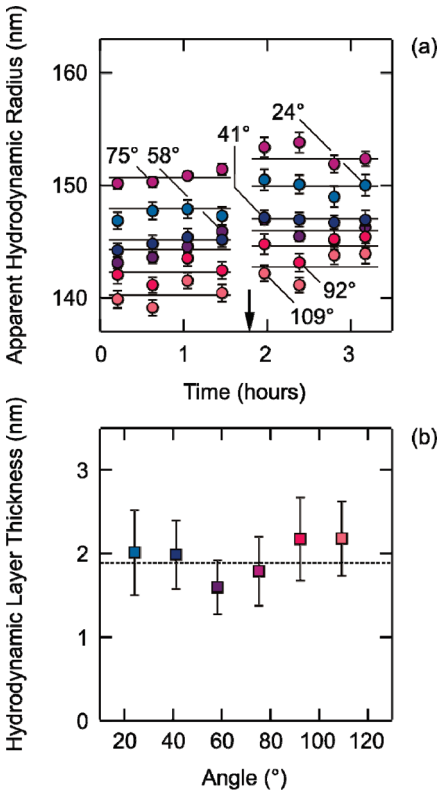

Figure 7. Layer thickness measured on multiangle goniometer in a stable suspension of SL-A latex particles at a particle concentration of 4.6×10^{12} m^{-3} (0.05 mg/L) and an ionic strength of 0.003 M with a subsequent addition of 600 mg/g LPEI. At this particle concentration, aggregation can be neglected. (a) Time dependence of the apparent hydrodynamic radius of the bare particle suspension with a subsequent addition of the polyelectrolyte (arrow). (b) Apparent layer thickness for the different angles measured.

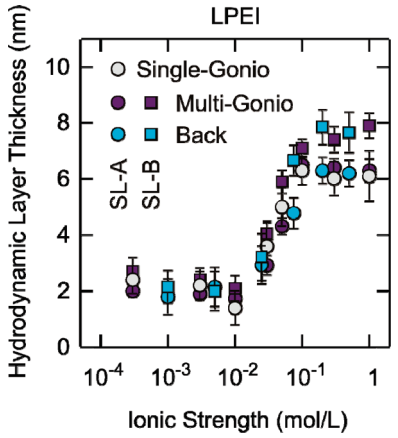

Figure 8. Hydrodynamic layer thickness of adsorbed LPEI as a function of the ionic strength measured with SL-A and SL-B particles with the multiangle goniometer and the backscattering instrument. The data are compared to single-angle measurements.

but due to the larger sensitivity of the instrument, such measurements can be still carried out down to particle concentrations of about 5×10^{10} m^{-3} (0.0005 mg/L).

These layer thickness measurements are also compared with similar measurements with SL-B particles. In this case, the particle concentration of SL-B was fixed at 1.8×10^{12} m^{-3} (0.1 mg/L), and the LPEI was added at a dose of 300 mg/g. Since these particles are larger than the SL-A particles, the form factor decays more strongly, and especially meaningful measurements cannot be carried out near the minima of the form factor. One also finds that the multiangle technique can be used down to concentrations of about 2×10^{11} m^{-3} (0.01 mg/L), while backscattering instrument still gives reasonable results down to concentrations of 8×10^{9} m^{-3} (0.0005 mg/L). The layer thickness and its ionic strength dependence are very similar for both particles. Again, one observes that the layer thickness increases roughly from 2 to 7 nm in a relatively narrow range of ionic strengths of 0.02−0.05 M.

Finding Optimal Conditions. The present experiments demonstrate that it is essential to carry layer thickness measurements below a particle number concentration of 10^{14} m^{-3}. The reason why the number concentration n turns out to be the important parameter is that this quantity determines the half-time of the aggregation[65]

$$T_{1/2} = \frac{2}{kn} \tag{2}$$

where k is the aggregation rate coefficient. Taking a typical value in fast aggregation conditions of $k \simeq 5 \times 10^{-18}$ m^3/s, one obtains $T_{1/2} \simeq 1$ h. In this time period, half of the particles would have aggregated under rapid aggregation conditions. Therefore, the particle concentration should be kept significantly below this number to avoid particle aggregate formation during the experiment.

When the particle concentration is decreased, the intensity of the scattering signal decreases as well. For the SL-A particles and single-angle goniometer, we find that reasonable count rates are still obtained for concentrations above 10^{12} m^{-3}. The larger SL-B particles can be still measured with the multiangle instrument at a particle concentration of about 10^{11} m^{-3}. When the number particle concentration is kept constant, the scattering signal at low scattering angles is proportional to the sixth power of the particle radius. As the particle size increases, a wider window of particles concentrations is available to perform the measurements. The smallest particle size that can be used for such measurements just yields sufficient scattering intensity at a particle concentration of 10^{14} m^{-3}. For both goniometer systems, this lower critical particle radius for poly(styrene) latex is about 100 nm, while for the backscattering instrument it is about 60 nm.

In principle, the same accuracy could be achieved at higher dilutions by increasing the measurement time. However, already the present experiments are relatively long, and one will rather consider shorter experiments at higher scattering intensities. For substantially larger particles, the scattering intensity becomes weak at larger scattering angles, especially close to the minima of the form factor, and the necessary accuracy in the radius measurement becomes difficult to achieve. We find that reliable layer thickness measurements are best carried out in the range of particle radii between 150 and 300 nm in the concentration range of 10^{12}−10^{13} m^{-3}. Clearly, the range further depends on the scattering properties of the material from which the particles are made from and on the sensitivity of the light scattering device. For substantially smaller particles, however, particle aggregation is extremely difficult to control.

Thickness of Adsorbed Polyelectrolyte Layers. With this reliable DLS technique at hand, the layer thickness of various polyelectrolytes adsorbed on oppositely charged particles was measured. The layer is fully developed in the saturated state, and its thickness strongly depends on the ionic strength. The available results are summarized in Figure 9. The present data are complemented with the recent measurements of PDADMAC layers on smaller sulfate latex particles.[36] We have equally included previous layer thickness measurements of adsorbed PSS films on

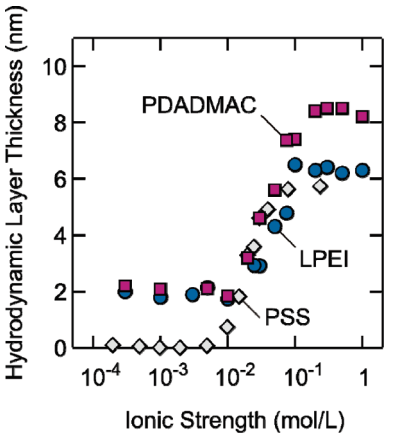

Figure 9. Hydrodynamic layer thickness of adsorbed polyelectrolyte layers on oppositely charged latex particles as a function of the ionic strength at pH 4.0. The cationic polyelectrolytes PDADMAC and LPEI were measured with the SL-A particles with backscattering and goniometer techniques. The anionic polyelectrolyte PSS was measured with amidine latex particles in a previous study.[59]

amidine latex particles,[59] even though these data are only trustworthy at higher ionic strengths.

The thickness of the adsorbed layers is always below 10 nm, and similar trends were observed for different polyelectrolytes. At low ionic strength, the adsorbed layer is extremely thin, typically around 1−2 nm. At higher ionic strengths, the layer is somewhat thicker, typically 6−9 nm. The transition between the two regimes is located in a relatively narrow range of ionic strengths of 0.01−0.05 M.

This increase in thickness with increasing ionic strength can be qualitatively rationalized by screening effects.[66−68] At low ionic strengths, the polyelectrolyte segments repel strongly, and the polyelectrolyte has a more rigid conformation. In this situation, the segment−surface interactions are strongly attractive and lead to flat adsorbed conformations. At higher ionic strengths, the repulsive interactions are progressively screened, which leads to more coiled conformations and thicker adsorbed layers. However, kinetic effects may also be important in determining the layer thickness.[69] Interestingly, polyelectrolyte brushes show the reverse trend as their thickness decreases with increasing ionic strength.[29,30]

4. Conclusion

Reliable layer thickness measurement of adsorbed polyelectrolytes on oppositely charged particles can be achieved with DLS, provided particle aggregation during these experiments is excluded. These effects are avoided by working at particle number concentrations $< 10^{14}$ m^{-3}, which assures that particle aggregation remains sufficiently slow. To maintain a sufficiently strong scattering intensity at these high dilutions, the particles must be chosen to be sufficiently large. For poly(styrene) latex particles, the best strategy consists in using particles with radii between 150 and 300 nm and to work in the concentration range $10^{12}-10^{13}$ m^{-3}. Under these conditions, the scattering intensity remains sufficiently high and the hydrodynamic radius can be measured with a precision < 0.3 nm. This precision is adequate to study the thickness of adsorbed layers down to the nanometer range. The multiangle goniometer method yields the most accurate results. Its advantage originates from the availability of up to eight independent measurements leading to better statistics than a single-angle instrument. The backscattering technique provides somewhat less precise measurements, but it offers a larger sensitivity at high dilution even for relatively small particles.

With these techniques at hand, adsorbed polyelectrolyte layers on oppositely charged particles are found to have thicknesses below 10 nm. At low ionic strengths, the layers are very thin, with thicknesses of 1−2 nm. At higher ionic strengths, the layers become somewhat thicker, having thicknesses of 6−9 nm. The transition between the thin and the thicker layer occurs in a relatively narrow range of ionic strengths, typically between 0.01 and 0.05 M. These observations were made with various cationic and anionic polyelectrolytes and can be thus considered as rather generic. We suspect that this transition originates from the progressive screening between the charged polyelectrolyte segments.

DLS provides excellent accuracy for hydrodynamic thickness measurements layers on colloidal particles provided particle aggregation is excluded during these experiments. The suitability of this technique was demonstrated by precise thickness measurements of nanometer-thick layers of adsorbed polyelectrolytes on oppositely charged particles. However, the technique is expected to be equally useful to study polyelectrolyte multilayers, adsorbed polymers in poor solvents, or layers of deposited nanoparticles.

Acknowledgment. This work was supported by the Swiss National Science Foundation and the University of Geneva.

References and Notes

(1) Howe, A. M.; Wesley, R. D.; Bertrand, M.; Cote, M.; Leroy, J. *Langmuir* **2006**, *22*, 4518–4525.
(2) van de Ven, T. G. M. *Adv. Colloid Interface Sci.* **2005**, *114*, 147–157.
(3) *Retention Aids*, 2nd ed.; Horn, D., Linhart, F., Eds.; Blackie Academic and Professional: London, 1996.
(4) Borkovec, M.; Papastavrou, G. *Curr. Opin. Colloid Interface Sci.* **2008**, *13*, 429–437.
(5) Caruso, F.; Caruso, R. A.; Möhwald, H. *Science* **1998**, *282*, 1111–1114.
(6) Estrela-Lopis, I.; Leporatti, S.; Moya, S.; Brandt, A.; Donath, E.; Möhwald, H. *Langmuir* **2002**, *18*, 7861–7866.
(7) Lichtenfeld, H.; Stechemesser, H.; Möhwald, H. *J. Colloid Interface Sci.* **2004**, *276*, 97–105.
(8) Blaakmeer, J.; Bohmer, M. R.; Cohen Stuart, M. A.; Fleer, G. J. *Macromolecules* **1990**, *23*, 2301–2309.
(9) Bohmer, M. R.; Heesterbeek, W. H. A.; Deratani, A.; Renard, E. *Colloids Surf., A* **1995**, *99*, 53–64.
(10) Killmann, E.; Bauer, D.; Fuchs, A.; Portenlanger, O.; Rehmet, R.; Rustemeier, O. *Prog. Colloid Polym. Sci.* **1998**, *111*, 135–143.
(11) Rustemeier, O.; Killmann, E. *J. Colloid Interface Sci.* **1997**, *190*, 360–370.
(12) Kleimann, J.; Gehin-Delval, C.; Auweter, H.; Borkovec, M. *Langmuir* **2005**, *21*, 3688–3698.
(13) Hoogendam, C. W.; de Keizer, A.; Cohen Stuart, M. A.; Bijsterbosch, B. H.; Batelaan, J. G.; van der Horst, P. M. *Langmuir* **1998**, *14*, 3825–3839.
(14) Liufu, S. C.; Xiao, H. N.; Li, Y. P. *J. Colloid Interface Sci.* **2005**, *285*, 33–40.
(15) Bonekamp, B. C.; Lyklema, J. *J. Colloid Interface Sci.* **1986**, *113*, 67–75.
(16) Furusawa, K.; Kanesaka, M.; Yamashita, S. *J. Colloid Interface Sci.* **1984**, *99*, 341–348.
(17) Jiang, M.; Popa, I.; Maroni, P.; Borkovec, M. *Colloids Surf., A* **2010**, *360*, 20–25.
(18) Vaccaro, A.; Hierrezuelo, J.; Skarba, M.; Galletto, P.; Kleimann, J.; Borkovec, M. *Langmuir* **2009**, *25*, 4864–4867.
(19) Barnett, K. G.; Cosgrove, T.; Vincent, B.; Burgess, A. N.; Crowley, T. L.; King, T.; Turner, J. D.; Tadros, T. F. *Polymer* **1981**, *22*, 283–285.
(20) Marshall, J. C.; Cosgrove, T.; Leermakers, F.; Obey, T. M.; Dreiss, C. A. *Langmuir* **2004**, *20*, 4480–4488.
(21) Hone, J. H. E.; Cosgrove, T.; Saphiannikova, M.; Obey, T. M.; Marshall, J. C.; Crowley, T. L. *Langmuir* **2002**, *18*, 855–864.
(22) Mears, S. J.; Cosgrove, T.; Obey, T.; Thompson, L.; Howell, I. *Langmuir* **1998**, *14*, 4997–5003.
(23) Zackrisson, M.; Stradner, A.; Schurtenberger, P.; Bergenholtz, J. *Langmuir* **2005**, *21*, 10835–10845.

(24) Cosgrove, T.; Obey, T.; Vincent, B. *J. Colloid Inteface Sci.* **1986**, *111*, 409–418.
(25) Roiter, Y.; Jaeger, W.; Minko, S. *Polymer* **2006**, *47*, 2493–2498.
(26) Popa, I.; Gillies, G.; Papastavrou, G.; Borkovec, M. *J. Phys. Chem. B* **2009**, *113*, 8458–8461.
(27) Pericet-Camara, R.; Papastavrou, G.; Borkovec, M. *Langmuir* **2004**, *20*, 3264–3270.
(28) Auroy, P.; Mir, Y.; Auvray, L. *Phys. Rev. Lett.* **1992**, *69*, 93–95.
(29) Guo, X.; Ballauff, M. *Langmuir* **2000**, *16*, 8719–8726.
(30) Guo, X.; Ballauff, M. *Phys. Rev. E* **2001**, *6405*, 051406.
(31) Ballauff, M. *Prog. Polym. Sci.* **2007**, *32*, 1135–1151.
(32) Cohen Stuart, M. A.; Waajen, F. H. W. H.; Cosgrove, T.; Vincent, B.; Crowley, T. L. *Macromolecules* **1984**, *17*, 1825–1830.
(33) Baker, J. A.; Berg, J. C. *Langmuir* **1988**, *4*, 1055–1061.
(34) Flood, C.; Cosgrove, T.; Howell, I.; Revell, P. *Langmuir* **2006**, *22*, 6923–6930.
(35) Min, G. K.; Bevan, M. A.; Prieve, D. C.; Patterson, G. D. *Colloids Surf., A* **2002**, *202*, 9–21.
(36) Bauer, D.; Buchhammer, H.; Fuchs, A.; Jaeger, W.; Killmann, E.; Lunkwitz, K.; Rehmet, R.; Schwarz, S. *Colloids Surf., A* **1999**, *156*, 291–305.
(37) Akari, S.; Schrepp, W.; Horn, D. *Ber. Bunsen-Ges. Phys. Chem.* **1996**, *100*, 1014–1016.
(38) Radeva, T.; Grozeva, M. *J. Colloid Interface Sci.* **2005**, *287*, 415–421.
(39) Lane, T. J.; Fletcher, W. R.; Gormally, M. V.; Johal, M. S. *Langmuir* **2008**, *24*, 10633–10636.
(40) Zhao, X. B.; Pan, F.; Coffey, P.; Lu, J. R. *Langmuir* **2008**, *24*, 13556–13564.
(41) Samoshina, Y.; Nylander, T.; Claesson, P.; Schillen, K.; Iliopoulos, I.; Lindman, B. *Langmuir* **2005**, *21*, 2855–2864.
(42) Sedeva, I. G.; Fornasiero, D.; Ralston, J.; Beattie, D. A. *Langmuir* **2009**, *25*, 4514–4521.
(43) Enarsson, L. E.; Wagberg, L. *Langmuir* **2008**, *24*, 7329–7337.
(44) Buron, C. C.; Filiatre, C.; Membrey, F.; Perrot, H.; Foissy, A. *J. Colloid Interface Sci.* **2006**, *296*, 409–418.
(45) Iruthayaraj, J.; Poptoshev, E.; Vareikis, A.; Makuska, R.; van der Wal, A.; Claesson, P. M. *Macromolecules* **2005**, *38*, 6152–6160.
(46) Rojas, O. J.; Claesson, P. M.; Muller, D.; Neuman, R. D. *J. Colloid Interface Sci.* **1998**, *205*, 77–88.
(47) Pericet-Camara, R.; Papastavrou, G.; Behrens, S. H.; Helm, C. A.; Borkovec, M. *J. Colloid Interface Sci.* **2006**, *296*, 496–506.
(48) Block, S.; Helm, C. A. *Phys. Rev. E* **2007**, *76*, 030801.
(49) Kirwan, L. J.; Maroni, P.; Behrens, S. H.; Papastavrou, G.; Borkovec, M. *J. Phys. Chem. B* **2008**, *112*, 14609–14619.
(50) Meszaros, R.; Thompson, L.; Bos, M.; de Groot, P. *Langmuir* **2002**, *18*, 6164–6169.
(51) Popa, I.; Cahill, B. P.; Maroni, P.; Papastavrou, G.; Borkovec, M. *J. Colloid Interface Sci.* **2007**, *309*, 28–35.
(52) Cahill, B. P.; Papastavrou, G.; Koper, G. J. M.; Borkovec, M. *Langmuir* **2008**, *24*, 465–473.
(53) Meszaros, R.; Varga, I.; Gilanyi, T. *Langmuir* **2004**, *20*, 5026–5029.
(54) Hansupalak, N.; Santore, M. M. *Langmuir* **2003**, *19*, 7423–7426.
(55) Kobayashi, M.; Juillerat, F.; Galletto, P.; Bowen, P.; Borkovec, M. *Langmuir* **2005**, *21*, 5761–5769.
(56) Lin, W.; Galletto, P.; Borkovec, M. *Langmuir* **2004**, *20*, 7465–7473.
(57) Bauer, D.; Killmann, E.; Jaeger, W. *Prog. Colloid Polym. Sci.* **1998**, *109*, 161–169.
(58) Hogg, R. V. *Am. Stat.* **1979**, *33*, 108–115.
(59) Gillies, G.; Lin, W.; Borkovec, M. *J. Phys. Chem. B* **2007**, *111*, 8626–8633.
(60) Yu, W. L.; Bouyer, F.; Borkovec, M. *J. Colloid Interface Sci.* **2001**, *241*, 392–399.
(61) Ashmore, M.; Hearn, J. *Langmuir* **2000**, *16*, 4906–4911.
(62) Walker, H. W.; Grant, S. B. *Colloids Surf., A* **1996**, *119*, 229–239.
(63) Popa, I.; Gillies, G.; Papastavrou, G.; Borkovec, M. *J. Phys. Chem. B* **2010**, *114*, 3170–3177.
(64) Hierrezuelo, J.; Vaccaro, A.; Borkovec, M. *J. Colloid Interface Sci.* **2010**, *347*, 202–208.
(65) Russel, W. B.; Saville, D. A.; Schowalter, W. R. *Colloidal Dispersions*; Cambridge University Press: Cambridge, 1989.
(66) Dobrynin, A. V.; Deshkovski, A.; Rubinstein, M. *Macromolecules* **2001**, *34*, 3421–3436.
(67) Netz, R. R.; Joanny, J. F. *Macromolecules* **1999**, *32*, 9013–9025.
(68) van de Steeg, H. G. M.; Cohen Stuart, M. A.; de Keizer, A.; Bijsterbosch, B. H. *Langmuir* **1992**, *8*, 2538–2546.
(69) O'Shaughnessy, B.; Vavylonis, D. *Eur. Phys. J. E* **2003**, *11*, 213–230.